14, which is then thresholded and the final decision is taken by the system as either 'Good', 'Acceptable' or 'Poor'.

In a fingerprint Image, the sweat pores exist on the ridges. Before describing the pore extraction method, it is necessary to know what a typical pore looks like. A typical average sized pore (in 500ppi fingerprint) may have gray levels as shown in Fig. 1. It has high (white to light gray) intensity value at the centre and low (gray to black) intensity around the centre pixel. When the image is inverted, the pores also get inverted, which can be then analyzed using the pore model as presented in [5], as shown in Fig. 3.

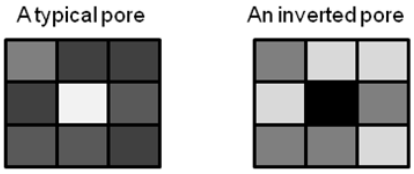

Figure 1. A typical Pore (in 3x3 neighborhood) and its inversion

The majority of pores within a 500 dpi image can be approximated using a slightly modified 2-dimensional Gaussian function as shown in equation (1) [5]:

$$M(x, y) = \quad (1)$$

The plot of the fingerprint pore model and the resulting 3 x 3 filter are shown in Figure 2 and Figure 3.

0.7569	0.6321	0.7569
0.6321	0	0.6321
0.7569	0.6321	0.7569

Figure 2. The 3 x 3 pore mask

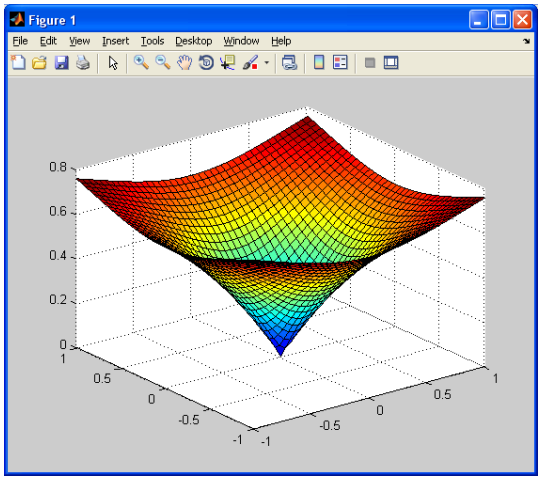

Figure 3. A 2-D Gaussian kernel as a pore model

An error map is generated which is given by equation (2) [5]:

$$E(x, y) = \sum_{i=x-r}^{x+r} \sum_{j=y-r}^{y+r} [(F(i, j) - M(i - x + r, j - y + r)]^2 \quad (2)$$

where, F(i, j) is the normalized value of the gray pixel between 0 and 1. Here, the lower the value of E(x, y) in equation (2), the stronger the pore remains. In other words, there remains a high probability of 3x3 region (with minimum value) to be a pore. Hence a low value of error means more chances of existence of pore.

A. Effective area (foreground) estimation and region of interest (ROI) determination

Foreground area is very important to evaluate (besides noise, dryness, wetness, scars/bruises etc.) the quality of the fingerprint images. It is difficult to pick up the details of the images if the foreground area is too small. A good quality image should have enough foreground area. So, we initiate the process with the foreground area calculation, which is defined as the percentage of the foreground blocks.

The effective foreground area (A_{eff}) is the ratio of foreground area (A_{fg}) as percentage of total area (A_{total}):

$$A_{eff}\% = (A_{fg}/A_{total}) * 100 \quad (3)$$

A smaller value of A_{eff} would mean a smaller area of fingerprint has been captured. For a given optimum threshold value T_{eff}, if $A_{eff} < T_{eff}$, the fingerprint image quality is declared "not good enough", which needs to be recaptured, refer to Fig. 20.

We propose a ROI-based quality estimation scheme, which comprises two phases: ROI determination and quality estimation of the area within ROI.

The analysis and evaluation process begins with the division of image under ROI into a set of disjoint blocks (w x w). The standard deviation of the gray scale values of the pixels in the k^{th} block (std_K) is then calculated using the equation (4) [2]. For a given optimum threshold value T_{std}, if $std_k(I) > T_{std}$, the block is declared "foreground block" or else "background block", refer to Fig. 5 (only ROI portion).

$$std_k(I) = \frac{1}{w^2}\sqrt{\sum_{i=-w/2}^{w/2}\sum_{j=-w/2}^{w/2}(I(i,j) - M(} \quad (4)$$

B. Quadrant analysis (QA) and quality index (QI) estimation

This novel approach is towards the projection and analysis of pores distribution in four quadrants. For any good quality print, the pores are generally found evenly distributed in all quadrants, which is not the case otherwise. Empirically determined optimum thresholds (in terms of percentage of pores) are specified and quality index is estimated declaring the image as good/acceptable/poor, refer to Fig. 4, 5 & 6.

Figure 4. Sample fingerprint: 012_3_1.tif [11]
(Cross Match Verifier 300 scanner at 500 dpi)

Pores are identified and marked with red bubbles, as shown Fig. 5. Not all the pores could be marked, as we need to change the value of 'r', which is the distance from the center of the pore model to the edge as well as the mask size (from 3x3 to 5x5 for r=2 and 7x7 for r=3), but otherwise most of them are located.

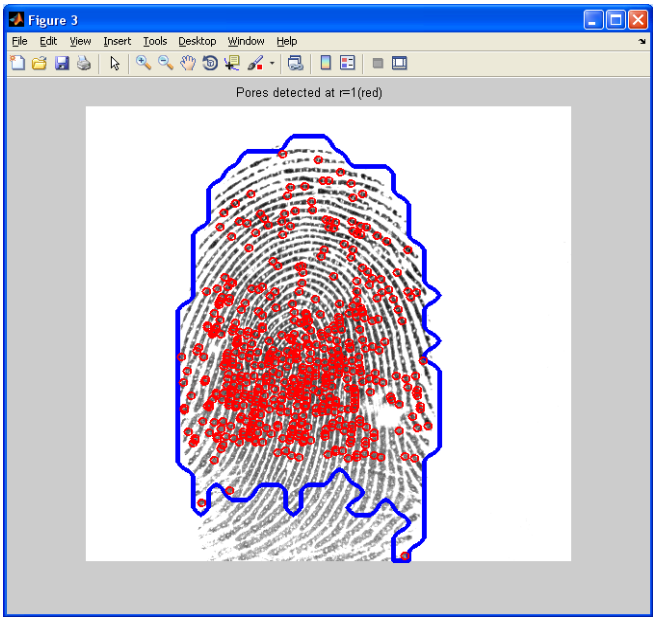

Figure 5. Pores Detection: 012_3_1.tif

To compute and plot the four quadrants for quadrant analysis, the pore locations within the ROI are identified and plotted using squared error method as given in equation (2). The centroid of the foreground region (within the ROI) is computed and then the quadrants are accurately and adaptively figured out. As can be evident from Fig. 16, 17, 21 and 22, for degraded quality prints, the pores distribution is seldom uniform in four logical regions.

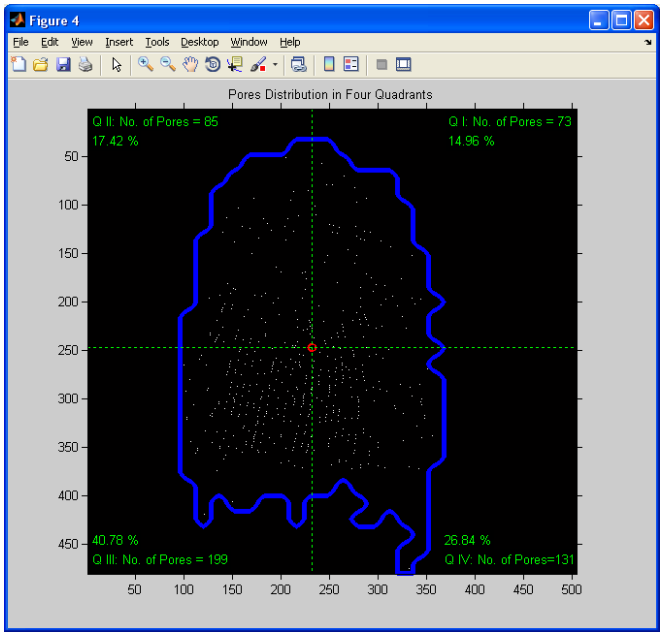

Figure 6. Quadrant Analysis: 012_3_1.tif
(slightly enlarged for a clear view)

C. *Pores Count*

This is a simple yet effective way of assessing the image quality from pores view-point, refers to the total count of identified pores in a given image, as shown in Fig. 7.

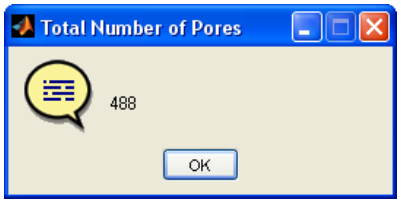

Figure 7. Pores Count: 012_3_1.tif

Empirically determined optimum thresholds (in terms of number of pores) are specified and quality index is estimated declaring the image as good/acceptable/poor.

D. *Pores Contrast (Michelson-based)*

This approach is all towards computing the pore-ridge contrast, which is based on Michelson contrast method [9]. Local contrast is computed using equation (5) for all the pores (and only the pores) in their local neighborhoods (here, 3x3), and a pore contrast image is generated, which is used further to classify pores into Strong/Average/Weak classes. Strong pores have been found exhibiting better reproducibility, as discussed in experimental results.

The image contrast is defined as relative local differences in pixel intensities. The definition is:

$$C_{Michelson} = (\qquad) \tag{5}$$

where, L_{max} is the maximum gray level and L_{min} is the minimum gray level in the image.

While computing, depending upon their respective intensities and threshold values, pores are categorized as: 'Strong', 'Average' and 'Weak' Pores, and are stored separately. Strong pores are characterized by high intensity values, average and weak ones with lesser values, refer to Fig. 8 and 9. As evident from the figures, we have very bright pixels (white, bright yellow etc.) referred to as Strong pores (with their known locations/indices). Similarly, average and weak pores are defined by relatively darker shades, refer to Fig. 16, 17, 18 and 19 for additional snapshots.

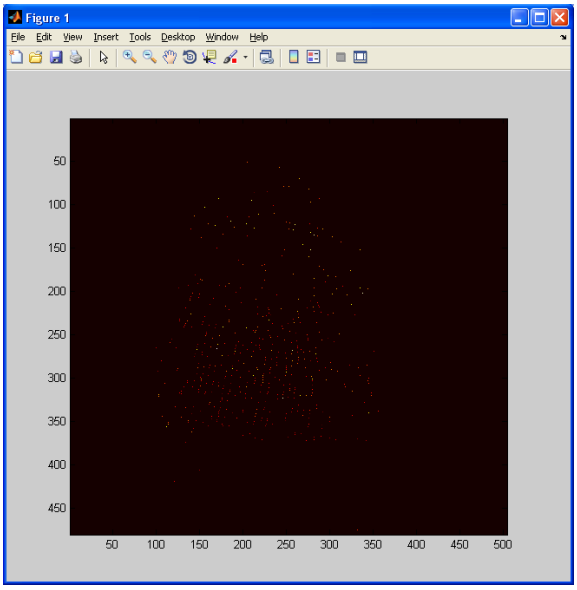

Figure 8. Pores contrast image: 012_3_1.tif

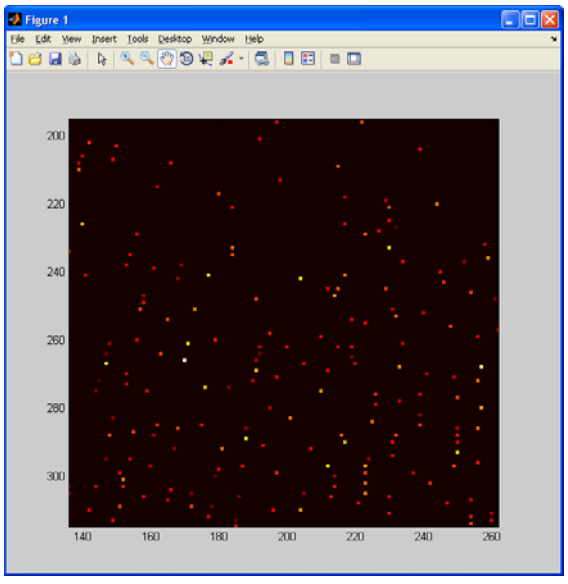

Figure 9. Magnified view of the 'pores contrast image': 012_3_1.tif

E. *Pores Strength*

As discussed in sec. II (preamble) and shown in Fig. 1. and 2., the lower the value of E(x,y), the stronger the pore is. In other words, there is a high probability of that 3x3 region to be a pore. Hence a low value of error means more chances of existence of pore.

Since information is related to probability in a similar manner i.e. low probability means more information, error value can give us information on existence of pore. To calculate the existence and strength of pore we first normalize the error value with its maximum possible value. Its maximum value will be generated when the pore has values as shown in Fig.10.

1	1	1
1	1	1
1	1	1

Figure 10. The 3 x 3 pore mask

This generates a $E_{max}(x, y) = 3.88979208$.

$$E_N(x, y) = E(x, y)/ E_{max}(x, y) \quad (6)$$

Where, $E_N(x, y)$ is the normalized error map with the values in the range 0 and 1. Now, the strength of pores can be calculated as:

$$S_p = \sum\sum (E_N(x,y))*\log_2(E_N(x,y)) /(\text{Number of Pores}) \quad (7)$$

over the entire image. A higher value means there is more possibility of existence of pores, and the pores strength is more.

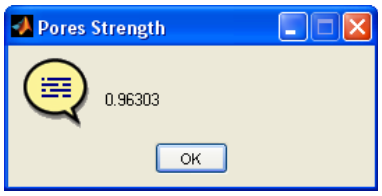

Figure 11. Pores Strength: 012_3_1.tif

This is how the image is analyzed from 'pores availability' point of view. Also, through a little strict thresholding, we may ensure a constellation of pores bearing relatively more strong pores, which may ensure better reproducibility and thus a higher pores matching accuracy. As far as quality index is concerned, depending upon the pores strength value and the corresponding thresholds, current image can be labeled as good (2)/acceptable (1)/poor (0).

F. *Fusion Engine*

The fusion engine combines the individual quality scores from different sub-systems and generates the final quality score, which are then used to adjudge the quality of the image, refer to Fig. 14 and 15.

*Fusion rule***.** The fusion rules adopted here for combining the available data are: the 'Weighted Sum Rule' [7][8].

- *Weighted* sum rule: In weighted sum rule (Ong et al., 2003; Nakagawa et al., 2006), a weighted factor is multiplied

with the score and then sum is calculated as given in equation (8).

$$f = \sum_{i=1}^{M} W_i x_i \quad (8)$$

Each submodule is assigned some weight, W_i, such that The submodule weights are calculated through empirical calculations, where weights are directly proportional to their respective sub-system's accuracy.

III. Experimental Results

Five quality measures have been selected and implemented in MATLAB. They are tested on images scanned with Cross Match Verifier 300 scanner at 500 dpi (pores are quite visible in these samples, as of now, no 1000ppi datasets are publicly available).

We have tested this module (Weighted Sum) over 15 images. We have presented experimental results to demonstrate the performance of the proposed multi-algorithm scheme, refer to Fig. 12 and 13. From the dataset, we have manually classified the images in three classes (i.e. good, acceptable and poor) based on their properties. The result (Fig. 12) shows that our method can distinguish the images as per their quality attributes with respect to level 3 sweat pores. The accuracy rate observed is 93.33%.

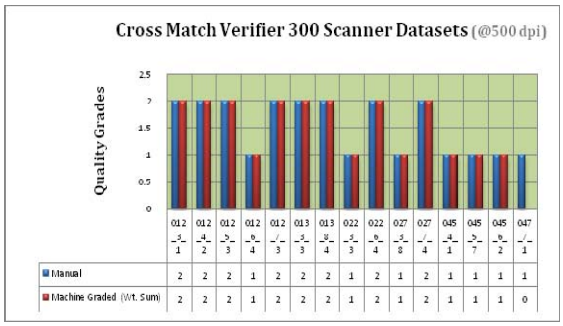

Figure 12. Experimental Results: manual vs machine grading

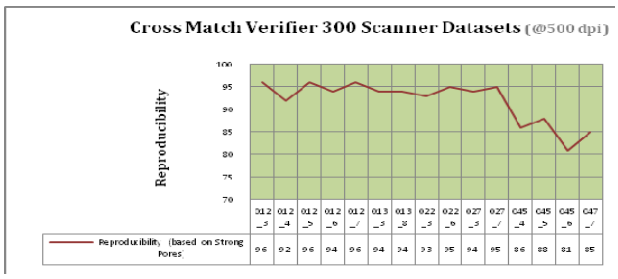

Figure 13. Experimental Results: Strong Pores Reproducibility

The result shown in Fig. 13, reveals the fact that the strong pores exhibit a good reproducibility of 91.93%. Here, same dataset is used, bearing 8 impressions per finger. The output (total number of strong pores identified and isolated) of the best image (out of 8) is considered as a reference image, and outputs from the rest 7 are then manually analyzed (over a range) with respect to the strong pores.

IV. Conclusion

In this paper, we have proposed a novel sweat pores-based quality assessment model for reliable estimation of fingerprint image quality from pores view-point. The proposed method spans across multiple measures with very high accuracy by analyzing primarily the micro characteristics of the image. Though the fusion scheme could perform extremely well over the small datasets presented here, it needs to be confirmed and tested rigorously over full range of other publicly available large datasets.

Acknowledgment

We wish to extend our sincere thanks to the Department of Information Technology (DIT), Ministry of Communications and Information Technology, Govt. of India, for assigning us this project and providing us an opportunity to contribute to security agencies within the country. Our thanks are also due to Ms. Pratibha Mokal, Ms. Anamika Singh and Mr. Varun Krishnan, C-DAC Mumbai, for their contributions towards the implementation of this quality assessment model.

References

[1] D. Maltoni, D. Maio, A. Jain, and S. Prabhakar, Handbook of Fingerprint Recognition. New York: Springer, 2003.

[2] M. Usman Akram, Sarwat Nasir, Anam Tariq, Irfan Zafar, Wasim Siddique Khan, "Improved Fingerprint Image Segmentation Using New Modified Gradient Based Technique", Proceedings of Canadian Conference on Electrical and Computer Engineering, pp. 1967-1972, 2008

[3] L. Hong, Y.Wan, and A. Jain, "Fingerprint image enhancement: Algorithm and performance evaluation," IEEE Trans. Pattern Anal. Mach. Intell., vol. 20, no. 8, pp. 777–789, Aug. 1998.

[4] Amar Khellaf, Azeddine Behgdadi, and Henri Dupoisot, "Entropic Contrast Enhancement" in IEEE transactions on medical Imaging,Vol. 10. No. 4,1991.

[5] M. Ray, P. Meenen, and R. Adhami. A novel approach to fingerprint pore extraction. Proc. Thirty-Seventh Southeastern Symposium on System Theory (SSST'05), pages 282–286, 2005.

[6] A. Rao, A Taxonomy for Texture Description and Identification. New York, NY: Springer-Verlag, 1990.

[7] Tejas Joshi, Somnath Dey and Debasis Samanta, "Multimodal biometrics: state of the art in fusion techniques", International Journal of Biometrics, Vol. 1, No. 4, pp. 393-417, 2009

[8] Toh, K-A, and Yau, W-Y, "Combination of hyperbolic functions for multimodal biometrics data fusion', IEEE Trans. On Systems, Man, and Cybernetics, Part B, vol. 34, no. 2, pp. 1196–1209, 2004.

[9] Martin Drahansky, "Experiments with Fingerprint Image Quality," bliss, pp.13-17, 2009 Symposium on Bio-inspired Learning and Intelligent Systems for Security, 2009

[10] Gonzalez Rafael C., Woods Richard E., "*Digital Image Processing*," 3rd edition. Prentice Hall, 2008.

[11] http://neurotechnology.com/download.html

[12] A.K. Jain, Y. Chen, and M. Demirkus, "Pores and Ridges: High-Resolution Fingerprint Matching Using Level 3 Features," IEEE Transactions on Pattern Analysis and Machine Intelligence, vol. 29, no. 1, pp. 15-27, 2007.

[13] http://www.biometricgroup.com/reports/public/NIJ_QRFRP_2007-DN-BX-K239_Final_Report.pdf

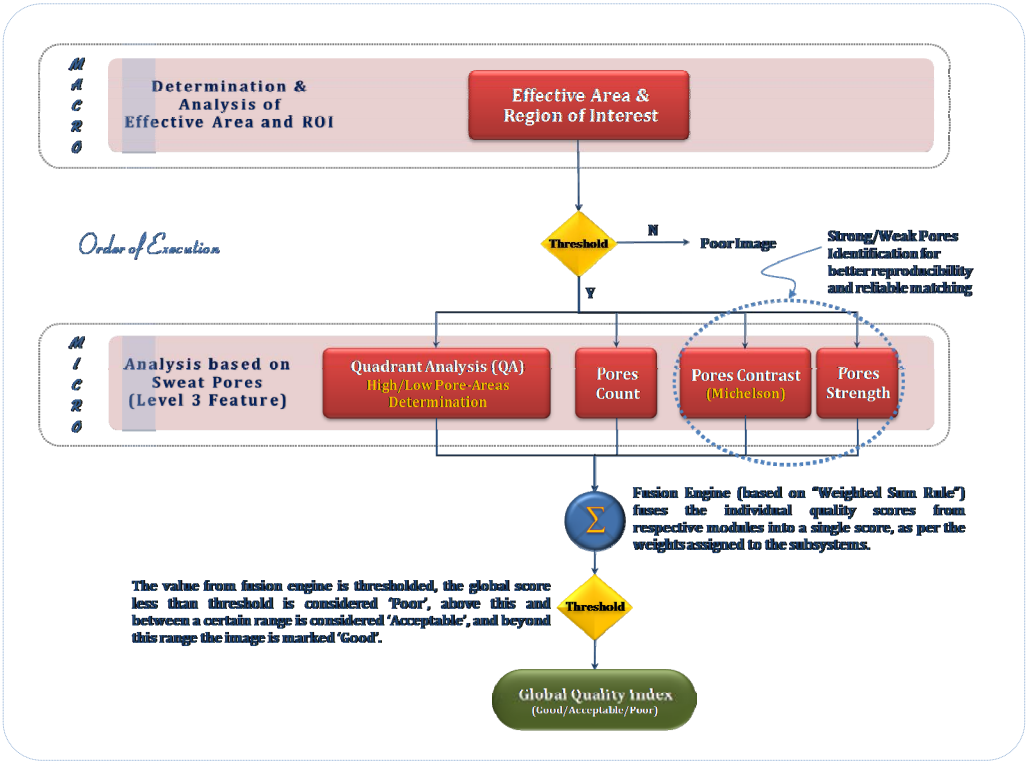

Figure 14. Sweat Pores-based Quality Assessment Scheme: Process Flow

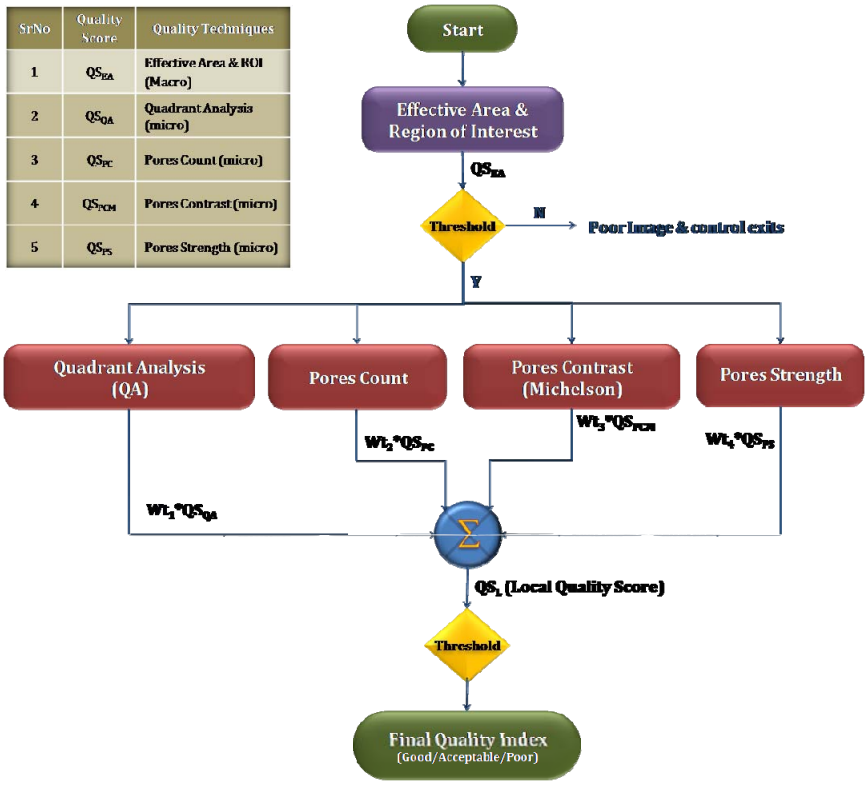

Figure 15. Sweat Pores-based Quality Assessment Scheme: Flow Chart

Figure 16. Sample Images (012_6_5.tif and 047_7_1.tif)

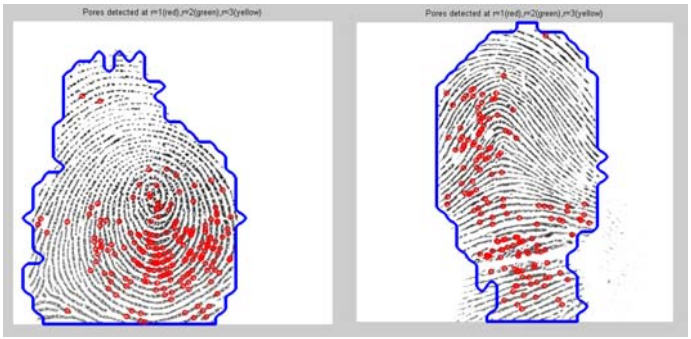

Figure 17. Detected Pores (slightly scaled) (012_6_5.tif and 047_7_1.tif)

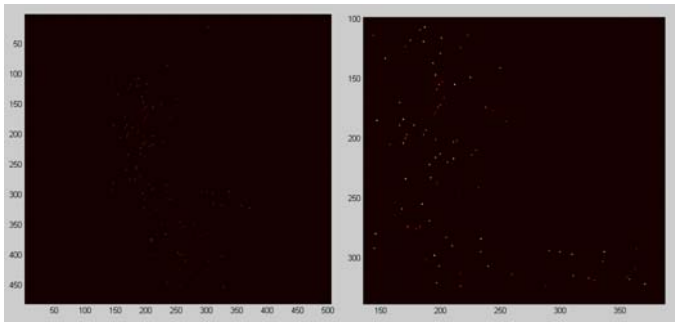

Figure 18. Pores Contrast Image: Unscaled & Scaled (047_7_1.tif)

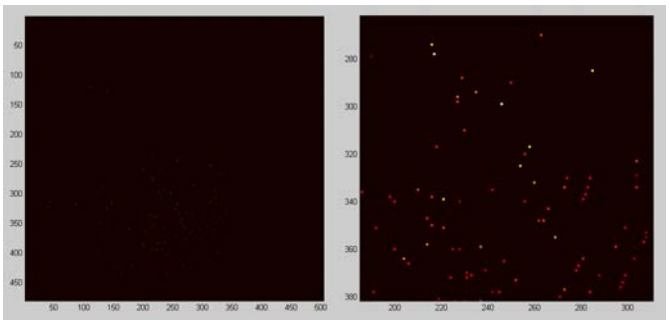

Figure 19. Pores Contrast Image: Unscaled & Scaled (012_6_5.tif)

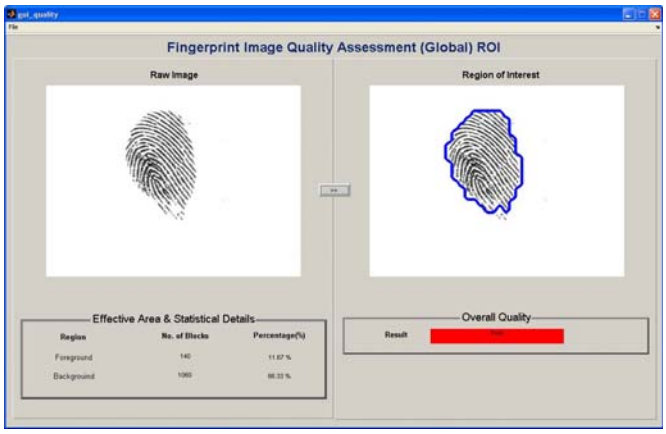

Figure 20. ROI-based fingerprint effective area calculation

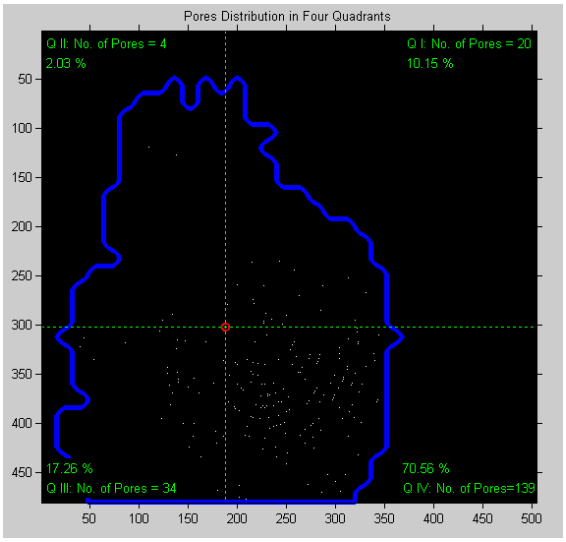

Figure 21. Pores Distribution (slightly scaled) (012_6_5.tif)

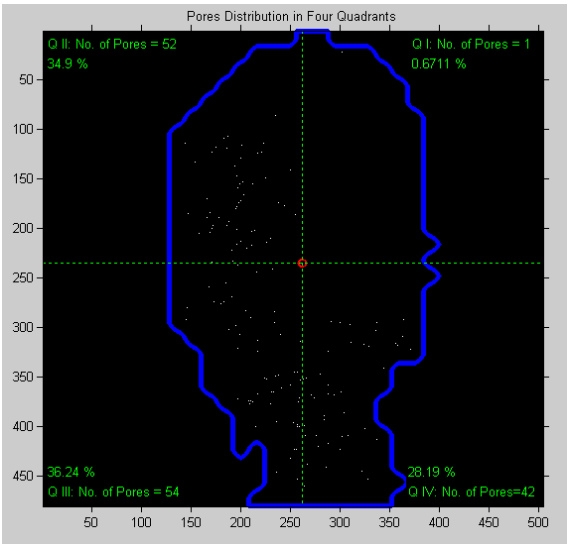

Figure 22. Pores Distribution (slightly scaled) (047_7_1.tif)